

Cryo-electron tomography of stationary phase *Burkholderia thailandensis*

Kanika Khanna^{1,2§}, Matthew D. Welch^{2§}

¹Gladstone Institute of Virology, Gladstone Institutes, San Francisco, California, United States

²Department of Molecular and Cell Biology, University of California, Berkeley, Berkeley, California, United States

§To whom correspondence should be addressed: kanika.khanna@gladstone.ucsf.edu; welch@berkeley.edu

Abstract

Burkholderia species belonging to the pseudomallei group include significant human and animal pathogens as well as the non-pathogenic species *Burkholderia thailandensis*. These bacteria co-opt the host cell machinery for their replication and spread between host cells. Thus, it is of interest to understand the structural features of these cells that contribute to host cell colonization and virulence. This study provides high-resolution cryo-electron tomograms of stationary phase *Burkholderia thailandensis*. It reveals the presence of compact nucleoids and storage granules, as well as examples of the type III secretion system and chemoreceptor arrays. The data can be used to investigate the near-atomic structure of stationary-phase bacterial macromolecules, such as ribosomes.

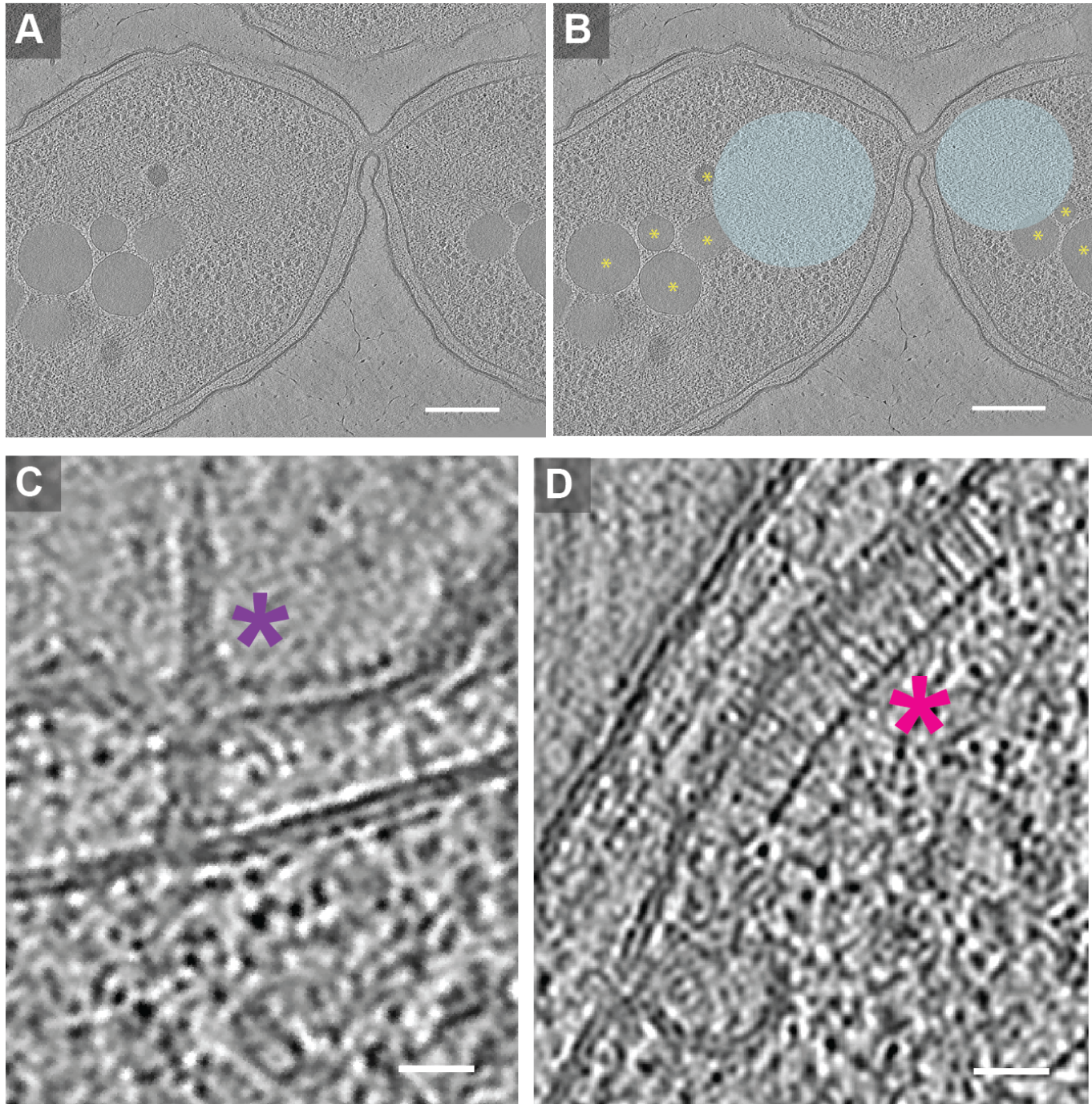


Figure 1.

Figure 1. Cryo-electron tomograms of stationary phase *B. thailandensis*. (A) Slice of a representative cryo-FIB milled tomogram of *B. thailandensis*. (B) Same as (A), annotated to depict storage granules (yellow asterisks) and condensed chromosomes segregating during cell division (blue). (C) Zoomed-in view of a *B. thailandensis* tomogram depicting a type III secretion system (purple asterisk). (D) Zoomed-in view of a *B. thailandensis* tomogram depicting chemoreceptor arrays (pink asterisk). Scale bars: (A,B): 200 nm (C,D): 25 nm.

Description

Burkholderia thailandensis has been used as a model to advance our understanding of related pathogenic pseudomallei-group *Burkholderia* species. These include *Burkholderia pseudomallei*, which causes melioidosis, a potentially fatal disease prevalent in tropical regions, and *B. mallei*, which causes glanders in horses and other related animals (Galyov, Brett, and

DeShazer 2010; Wiersinga et al. 2018; Khan et al. 2013). Currently, there are no vaccines for disease prevention (Titball et al. 2017), and infections caused by these bacteria are difficult to treat as they are resistant to many antibiotics (Rhodes and Schweizer 2016). These Gram-negative facultative intracellular bacteria use virulence factors to hijack the host cellular machinery for replication and spread from cell to cell (Galyov, Brett, and DeShazer 2010; Willcocks et al. 2016). While *B. thailandensis* encodes similar virulence factors (Haraga et al. 2008; Brett, DeShazer, and Woods 1998), it is rarely pathogenic to humans (Glass et al. 2006), making it a valuable model for studying the intracellular life cycle of pseudomallei-group *Burkholderia* in the laboratory.

Pseudomallei-group *Burkholderia* species are distinctive among bacterial pathogens in that they induce cell-cell fusion to spread between cells in tissues, forming multinucleate giant cells (MNGCs) (Kespichayawattana et al. 2000). To do so, they require two activities. One is bacterial motility, either actin-based or flagellar (Benanti, Nguyen, and Welch 2015; Kespichayawattana et al. 2000; French et al. 2011; Toesca, French, and Miller 2014). The other is the function of a type VI secretion system (T6SS), specifically T6SS-5 (Toesca, French, and Miller 2014; French et al. 2011; Kostow and Welch 2022; Schwarz et al. 2014), a needle-like apparatus that secretes bacterial effector proteins from its tip (Jurėnas and Journet 2021). *B. thailandensis*-induced cell-cell fusion occurs within host cell plasma membrane protrusions (Kostow and Welch 2022) and requires T6SS-5 spike proteins VgrG5 (Schwarz et al. 2014; Toesca, French, and Miller 2014) and TagD5 (Kostow and Welch 2022).

We set out to visualize *B. thailandensis* cell structures at a high resolution using cryo-electron tomography (cryo-ET) coupled with cryo-focused ion beam milling (cryo-FIB) (Khanna and Villa 2022; Keck, Enninga, and Swistak 2023) (see *Methods*). We were particularly interested in visualizing the T6SS machinery, which was previously visualized by cryo-ET in *Vibrio cholerae* (Basler et al. 2012) and *Myxococcus xanthus* (Chang et al. 2017) and appears as cytoplasmic tubes resembling bacteriophage tails that are perpendicularly anchored in the bacterial membranes. To specifically visualize T6SS-5, we used *B. thailandensis* strain E264 Δ T6SS-1,2,4,6, which was engineered with inactivating mutations in T6SS-1, 2, 4, and 6, leaving only T6SS-5 active (Schwarz et al. 2010). The expression of *B. thailandensis* T6SS-5 is tightly controlled and induced exclusively inside host cells (Chen et al. 2011; Lennings, West, and Schwarz 2018; Schwarz et al. 2014). VirA, the principal regulator of T6SS-5 expression, senses the presence of reduced glutathione (GSH) in the host cytosol, initiating the expression of T6SS-5 genes (Wong, Chen, and Gan 2015). This knowledge can be leveraged to express T6SS-5 genes in *B. thailandensis* grown in broth culture without host cells by supplementing the media with GSH (Wong, Chen, and Gan 2015; Kostow and Welch 2022). Hence, we decided to use cryo-FIB-ET to visualize *B. thailandensis* grown in broth with GSH to increase the chances of visualizing T6SS-5.

We acquired 13 high-quality tomograms of *B. thailandensis*. All of our tomograms displayed characteristics typical of stationary-phase bacteria (Figure 1). This includes the presence of condensed DNA (Bauda et al. 2024), which is suggested to serve as a strategy to safeguard DNA from potential damage (Lee et al. 2015; Almiron et al. 1992; Janissen et al. 2018). It also includes the presence of other spherical structures, potentially either polyphosphate (polyP) or polyhydroxyalkanoate (PHA) granules (Racki et al. 2017; Chawla et al. 2023; Achbergerová and Nahálka 2011; Tocheva et al. 2013). These presumed PolyP/PHA granules exhibited irregular shapes and heterogeneity in size, ranging from approximately 50 to 400 nm. The granules also varied in number and were located non-uniformly within the cell. Other observed structures include numerous ribosomes, chromosome segregation during the final stages of cell division (Figure 1A,B), an instance of the type III secretion system (T3SS) (Figure 1C), and an instance of chemoreceptor arrays (Figure 1D).

Regrettably, we did not visualize T6SS-5 in our dataset. Several possibilities may explain our inability to visualize T6SS-5. Firstly, the limited sample size and the thinning of cells (to \sim 200 nm) during cryo-FIB milling, allowing us to capture only \sim 20% of the cell, could have contributed to the inability to observe individual examples of T6SS-5. Increased data acquisition might address this limitation. Consistent with this notion, a prior study detected the T6SS in whole *M. xanthus* cells in only 53 out of 1650 tomograms (\sim 3.2%), suggesting a low probability of detecting T6SS in cells in general (Chang et al. 2017). In the future, we anticipate that using correlative light microscopy to identify cells expressing T6SS-5 in *B. thailandensis* can help alleviate this issue. Secondly, while the expression of VgrG-5 was observed under our growth conditions by western blotting (Kostow and Welch 2022), this might not necessarily correspond to the assembly of the complete T6SS-5 apparatus, which may depend on factors beyond the addition of GSH to the growth media. Lastly, it is plausible that optimizing our growth conditions to ensure bacterial cells are not in the stationary phase when GSH is introduced to the media could enhance our ability to visualize T6SS-5.

Nevertheless, we anticipate that these tomograms will be a valuable resource for the scientific community interested in studying bacterial structures for cells in stationary phase, for example, in deciphering the structure of stationary-phase ribosomes. We have deposited binned tomograms in the Electron Microscopy Data Bank (EMDB) with accession code EMD-

44416 and aligned tilt series in the Electron Microscopy Public Image Archive (EMPIAR) database with accession code EMPIAR-11957.

Methods

Bacterial cell culture

B. thailandensis E264 Δ T6SS-1,2,4,6 strain was generously provided by the lab of Joseph D. Mougous (Schwarz et al. 2010). For expression of VgrG5 in broth, the same procedure was followed as was previously reported (Kostow and Welch 2022). Briefly, *B. thailandensis* was grown overnight in LB broth, followed by 1:10 dilution in the morning. After 2 h, cultures were split into two tubes with 2 mM reduced L-glutathione (GSH, Sigma-Aldrich, G4251) added in one of them. Cultures were further grown for 4 h for cryo-ET, as described below.

Tomography Sample Preparation and Data Acquisition

Holey carbon-coated QUANTIFOIL® R 2/1 copper grids (Electron Microscopy Sciences, Q350CR1) were glow-discharged using Pelco easiGlow™ Glow Discharge Cleaning System, and 6 μ l of GSH-induced *B. thailandensis* culture was deposited on each grid. The sample was blotted from the side of the grid opposite to the cells using Whatman No. 1 filter paper to remove excess liquid such that cells form a monolayer on the grid. Vitrification was done in liquid ethane using a manual freeze-plunger at the Donner Cryo-EM Facility, Lawrence Berkeley National Laboratory (LBNL). The samples were stored in liquid nitrogen until further use.

Subsequently, for cryo-FIB milling, vitrified cells were transported to the Stanford-SLAC CryoET Specimen Preparation Center and milled using Aquilos 2 cryo-FIB (ThermoFisher Scientific) manually, as described in previous workflows (Wagner et al. 2020; Khanna et al. 2021). Briefly, grids were sputter-coated with metallic platinum, followed by coating with a ~500 nm organometallic platinum layer using a gas injection system and another round of sputter-coating with metallic platinum. Lamellae with thickness ranging from ~150-200 nm were prepared using a 30 kV focused ion beam, gradually reducing the beam current from 500 pA (rough milling) to 10 pA (polishing). Micro-expansion joints were also milled to prevent lamellae bending and fracture (Wolff et al. 2019).

Milled samples were transported to UW-Madison Cryo-Electron Microscopy Research Center (CEMRC) for cryo-ET data acquisition using 300 kV Titan Krios transmission electron microscope (ThermoFisher Scientific) equipped with a K3 camera and an energy filter (both from Gatan). A slit width of 20 eV was used for data acquisition in 0.5 binning mode on the K3 detector. SerialEM 4.1 software was used for data acquisition (Mastronarde 2005). Tilt series were acquired at 3.726 Å pixel size using a dose-symmetric (Hagen, Wan, and Briggs 2017) scheme with 3° increments starting from 0° relative to the lamella pretilt, with the total dose applied to the sample ranging from 70-80 e-/Å² and a defocus of -5 μ m. MotionCor2 was used to correct individual tilt frames (Zheng et al. 2017) and AreTomo for tilt-series alignment and reconstruction with dose weighting (Zheng et al. 2022). Final reconstruction and visualization was done using the patch-tracking method in IMOD 4.11 (Kremer, Mastronarde, and McIntosh 1996).

Acknowledgements:

We thank Welch lab members, especially Nora Kostow, whose previous work supported this project. We thank Dr. Agustin Avila Sakar at the LBNL cryo-EM facility in Donner Hall for assistance with the manual plunger, Dr. Lydia-Marie Joubert at the Stanford-SLAC CryoET Specimen Preparation Center for assistance with cryo-FIB milling, and Dr. Jae Yang and Anil Kumar at the Midwest Center for Cryo-ET (MCCET) for assistance with cryo-ET data acquisition. We thank Joseph D. Mougous for the gift of *B. thailandensis* Δ t6ss-1,2,4,6 strain.

References

- Achbergerová L, Nahálka J. 2011. Polyphosphate--an ancient energy source and active metabolic regulator. *Microb Cell Fact* 10: 63. PubMed ID: [21816086](#)
- Almirón M, Link AJ, Furlong D, Kolter R. 1992. A novel DNA-binding protein with regulatory and protective roles in starved *Escherichia coli*. *Genes Dev* 6(12B): 2646-54. PubMed ID: [1340475](#)
- Basler M, Pilhofer M, Henderson GP, Jensen GJ, Mekalanos JJ. 2012. Type VI secretion requires a dynamic contractile phage tail-like structure. *Nature* 483(7388): 182-6. PubMed ID: [22367545](#)
- Bauda E, Gallet B, Moravcova J, Effantin G, Chan H, Novacek J, et al., Morlot C. 2024. Ultrastructure of macromolecular assemblies contributing to bacterial spore resistance revealed by in situ cryo-electron tomography. *Nat Commun* 15(1): 1376. PubMed ID: [38355696](#)

- Benanti EL, Nguyen CM, Welch MD. 2015. Virulent Burkholderia species mimic host actin polymerases to drive actin-based motility. *Cell* 161(2): 348-60. PubMed ID: [25860613](#)
- Brett PJ, DeShazer D, Woods DE. 1998. Burkholderia thailandensis sp. nov., a Burkholderia pseudomallei-like species. *Int J Syst Bacteriol* 48 Pt 1: 317-20. PubMed ID: [9542103](#)
- Chang YW, Rettberg LA, Ortega DR, Jensen GJ. 2017. In vivo structures of an intact type VI secretion system revealed by electron cryotomography. *EMBO Rep* 18(7): 1090-1099. PubMed ID: [28487352](#)
- Chawla R, Tom JKA, Boyd T, Grotjahn DA, Park D, Deniz AA, Racki LR. 2023. Reentrant DNA shells tune polyphosphate condensate size. *bioRxiv*. PubMed ID: [37745474](#)
- Chen Y, Wong J, Sun GW, Liu Y, Tan GY, Gan YH. 2011. Regulation of type VI secretion system during Burkholderia pseudomallei infection. *Infect Immun* 79(8): 3064-73. PubMed ID: [21670170](#)
- French CT, Toesca IJ, Wu TH, Teslaa T, Beaty SM, Wong W, et al., Miller JF. 2011. Dissection of the Burkholderia intracellular life cycle using a photothermal nanoblade. *Proc Natl Acad Sci U S A* 108(29): 12095-100. PubMed ID: [21730143](#)
- Galyov EE, Brett PJ, DeShazer D. 2010. Molecular insights into Burkholderia pseudomallei and Burkholderia mallei pathogenesis. *Annu Rev Microbiol* 64: 495-517. PubMed ID: [20528691](#)
- Glass MB, Gee JE, Steigerwalt AG, Cavuoti D, Barton T, Hardy RD, et al., Wilkins PP. 2006. Pneumonia and septicemia caused by Burkholderia thailandensis in the United States. *J Clin Microbiol* 44(12): 4601-4. PubMed ID: [17050819](#)
- Hagen WJH, Wan W, Briggs JAG. 2017. Implementation of a cryo-electron tomography tilt-scheme optimized for high resolution subtomogram averaging. *J Struct Biol* 197(2): 191-198. PubMed ID: [27313000](#)
- Haraga A, West TE, Brittnacher MJ, Skerrett SJ, Miller SI. 2008. Burkholderia thailandensis as a model system for the study of the virulence-associated type III secretion system of Burkholderia pseudomallei. *Infect Immun* 76(11): 5402-11. PubMed ID: [18779342](#)
- Janissen R, Arens MMA, Vtyurina NN, Rivai Z, Sunday ND, Eslami-Mossallam B, et al., Meyer AS. 2018. Global DNA Compaction in Stationary-Phase Bacteria Does Not Affect Transcription. *Cell* 174(5): 1188-1199.e14. PubMed ID: [30057118](#)
- Jurėnas D, Journet L. 2021. Activity, delivery, and diversity of Type VI secretion effectors. *Mol Microbiol* 115(3): 383-394. PubMed ID: [33217073](#)
- Keck C, Enninga J, Swistak L. 2023. Caught in the act: In situ visualization of bacterial secretion systems by cryo-electron tomography. *Mol Microbiol*. PubMed ID: [37975530](#)
- Kespichayawattana W, Rattanachetkul S, Wanun T, Utaisincharoen P, Sirisinha S. 2000. Burkholderia pseudomallei induces cell fusion and actin-associated membrane protrusion: a possible mechanism for cell-to-cell spreading. *Infect Immun* 68(9): 5377-84. PubMed ID: [10948167](#)
- Khan I, Wieler LH, Melzer F, Elschner MC, Muhammad G, Ali S, et al., Saqib M. 2013. Glanders in animals: a review on epidemiology, clinical presentation, diagnosis and countermeasures. *Transbound Emerg Dis* 60(3): 204-21. PubMed ID: [22630609](#)
- Khanna K, Lopez-Garrido J, Sugie J, Pogliano K, Villa E. 2021. Asymmetric localization of the cell division machinery during Bacillus subtilis sporulation. *Elife* 10. PubMed ID: [34018921](#)
- Khanna K, Villa E. 2022. Revealing bacterial cell biology using cryo-electron tomography. *Curr Opin Struct Biol* 75: 102419. PubMed ID: [35820259](#)
- Kostow N, Welch MD. 2022. Plasma membrane protrusions mediate host cell-cell fusion induced by Burkholderia thailandensis. *Mol Biol Cell* 33(8): ar70. PubMed ID: [35594178](#)
- Kremer JR, Mastronarde DN, McIntosh JR. 1996. Computer visualization of three-dimensional image data using IMOD. *J Struct Biol* 116(1): 71-6. PubMed ID: [8742726](#)
- Lee SY, Lim CJ, Dröge P, Yan J. 2015. Regulation of Bacterial DNA Packaging in Early Stationary Phase by Competitive DNA Binding of Dps and IHF. *Sci Rep* 5: 18146. PubMed ID: [26657062](#)
- Lennings J, West TE, Schwarz S. 2018. The Burkholderia Type VI Secretion System 5: Composition, Regulation and Role in Virulence. *Front Microbiol* 9: 3339. PubMed ID: [30687298](#)
- Mastronarde DN. 2005. Automated electron microscope tomography using robust prediction of specimen movements. *J Struct Biol* 152(1): 36-51. PubMed ID: [16182563](#)

- Racki LR, Tocheva EI, Dieterle MG, Sullivan MC, Jensen GJ, Newman DK. 2017. Polyphosphate granule biogenesis is temporally and functionally tied to cell cycle exit during starvation in *Pseudomonas aeruginosa*. *Proc Natl Acad Sci U S A* 114(12): E2440-E2449. PubMed ID: [28265086](#)
- Rhodes KA, Schweizer HP. 2016. Antibiotic resistance in *Burkholderia* species. *Drug Resist Updat* 28: 82-90. PubMed ID: [27620956](#)
- Schwarz S, Singh P, Robertson JD, LeRoux M, Skerrett SJ, Goodlett DR, West TE, Mougous JD. 2014. VgrG-5 is a *Burkholderia* type VI secretion system-exported protein required for multinucleated giant cell formation and virulence. *Infect Immun* 82(4): 1445-52. PubMed ID: [24452686](#)
- Schwarz S, West TE, Boyer F, Chiang WC, Carl MA, Hood RD, et al., Mougous JD. 2010. *Burkholderia* type VI secretion systems have distinct roles in eukaryotic and bacterial cell interactions. *PLoS Pathog* 6(8): e1001068. PubMed ID: [20865170](#)
- Titball RW, Burtneck MN, Bancroft GJ, Brett P. 2017. *Burkholderia pseudomallei* and *Burkholderia mallei* vaccines: Are we close to clinical trials? *Vaccine* 35(44): 5981-5989. PubMed ID: [28336210](#)
- Tocheva EI, Dekas AE, McGlynn SE, Morris D, Orphan VJ, Jensen GJ. 2013. Polyphosphate storage during sporulation in the gram-negative bacterium *Acetonebacterium longum*. *J Bacteriol* 195(17): 3940-6. PubMed ID: [23813732](#)
- Toesca JJ, French CT, Miller JF. 2014. The Type VI secretion system spike protein VgrG5 mediates membrane fusion during intercellular spread by pseudomallei group *Burkholderia* species. *Infect Immun* 82(4): 1436-44. PubMed ID: [24421040](#)
- Wagner FR, Watanabe R, Schampers R, Singh D, Persoon H, Schaffer M, et al., Villa E. 2020. Preparing samples from whole cells using focused-ion-beam milling for cryo-electron tomography. *Nat Protoc* 15(6): 2041-2070. PubMed ID: [32405053](#)
- Wiersinga WJ, Virk HS, Torres AG, Currie BJ, Peacock SJ, Dance DAB, Limmathurotsakul D. 2018. Melioidosis. *Nat Rev Dis Primers* 4: 17107. PubMed ID: [29388572](#)
- Willcocks SJ, Denman CC, Atkins HS, Wren BW. 2016. Intracellular replication of the well-armed pathogen *Burkholderia pseudomallei*. *Curr Opin Microbiol* 29: 94-103. PubMed ID: [26803404](#)
- Wolff G, Limpens RWAL, Zheng S, Snijder EJ, Agard DA, Koster AJ, Bárcena M. 2019. Mind the gap: Micro-expansion joints drastically decrease the bending of FIB-milled cryo-lamellae. *J Struct Biol* 208(3): 107389. PubMed ID: [31536774](#)
- Wong J, Chen Y, Gan YH. 2015. Host Cytosolic Glutathione Sensing by a Membrane Histidine Kinase Activates the Type VI Secretion System in an Intracellular Bacterium. *Cell Host Microbe* 18(1): 38-48. PubMed ID: [26094804](#)
- Zheng SQ, Palovcak E, Armache JP, Verba KA, Cheng Y, Agard DA. 2017. MotionCor2: anisotropic correction of beam-induced motion for improved cryo-electron microscopy. *Nat Methods* 14(4): 331-332. PubMed ID: [28250466](#)
- Zheng S, Wolff G, Greenan G, Chen Z, Faas FGA, Bárcena M, et al., Agard DA. 2022. AreTomo: An integrated software package for automated marker-free, motion-corrected cryo-electron tomographic alignment and reconstruction. *J Struct Biol X* 6: 100068. PubMed ID: [35601683](#)

Funding:

This work was funded by Grant R35 GM127108 from the NIH/NIGMS to Matthew D. Welch. Kanika Khanna was a Simons Foundation Awardee of the Life Sciences Research Foundation. Some of this work was performed at the Stanford-SLAC CryoET Specimen Preparation Center (SCSC), and the Midwest Center for Cryo-Electron Tomography (MCCET) and the Cryo-EM Research Center located in the Department of Biochemistry at the University of Wisconsin-Madison, supported by the National Institutes of Health Common Fund's Transformative High Resolution Cryo-electron Microscopy Program (U24 GM139166 and U24 GM139168).

Supported by National Institutes of Health (United States) R35 GM127108 to Matthew D. Welch.

Supported by National Institutes of Health (United States) U24 GM139166 to Stanford-SLAC CryoET Specimen Preparation Service Center.

Supported by National Institutes of Health (United States) U24 GM139168 to Midwest Center for Cryo-Electron Tomography

Author Contributions: Kanika Khanna: conceptualization, data curation, formal analysis, funding acquisition, investigation, methodology, resources, validation, visualization, writing - original draft, writing - review editing. Matthew D. Welch: conceptualization, funding acquisition, project administration, supervision, writing - review editing.

Reviewed By: Anonymous

4/24/2024 - Open Access

History: **Received** March 11, 2024 **Revision Received** April 18, 2024 **Accepted** April 22, 2024 **Published Online** April 24, 2024 **Indexed** May 8, 2024

Copyright: © 2024 by the authors. This is an open-access article distributed under the terms of the Creative Commons Attribution 4.0 International (CC BY 4.0) License, which permits unrestricted use, distribution, and reproduction in any medium, provided the original author and source are credited.

Citation: Khanna, K; Welch, MD (2024). Cryo-electron tomography of stationary phase *Burkholderia thailandensis*. microPublication Biology. [10.17912/micropub.biology.001178](https://doi.org/10.17912/micropub.biology.001178)